Ultramicroscopy 30 (1989) 429–434
North-Holland, Amsterdam

SHORT NOTE

THE SPECTRAL SIGNAL-TO-NOISE RATIO RESOLUTION CRITERION: COMPUTATIONAL EFFICIENCY AND STATISTICAL PRECISION

Michael UNSER *,**

Biomedical Engineering and Instrumentation Branch, National Institutes of Health, Bethesda, Maryland 20892, USA

Benes L. TRUS

Computer Systems Laboratory, Division of Computer Research and Technology, National Institutes of Health, Bethesda, Maryland 20892, USA

Joachim FRANK

Wadsworth Center for Laboratories and Research, New York State Department of Health, Albany, New York 12201, USA

and

Alasdair C. STEVEN

Laboratory of Physical Biology, National Institute of Arthritis, Musculoskeletal and Skin Diseases, National Institutes of Health, Bethesda, Maryland 20892, USA

Received 14 March 1989

This note describes a practical improvement in the computational efficiency of the spectral signal-to-noise ratio (SSNR) resolution criterion for correlation-averaged images. The total set of N images is randomly partitioned into n_g subsets, each subset is separately averaged, and a reduced form of the SSNR is computed from these average images. In general, larger values of n_g achieve lower statistical uncertainty, while smaller values of n_g are computationally more expedient. It is shown that, for negatively stained data, a judicious compromise is achieved with $10 \leq n_g \leq 20$, regardless of how large N may be.

1. Introduction

In a previous paper [1], we have introduced the SSNR resolution criterion. Compared with three alternative criteria, viz. the differential phase residual (DPR) [2], the Fourier ring correlation (FRC) [3], and the Q-factor [4], the SSNR offers several advantages. First, it relates in a straightforward way to the diffraction-based resolution criterion that has long been applied to crystalline specimens [5]. Second, it has a lower statistical uncertainty than the DPR, the FRC, or the Q-factor (which is usually computed for single Fourier components). Third, it allows one to estimate the improvement of resolution that may be expected from expanding the data set by a specific amount, as well as the asymptotic resolution to be achieved by averaging over an infinitely large data set.

However, whereas the DPR and FRC are calculated on the basis of two Fourier transforms – one for each partial average over the respective halves of the data set – the SSNR requires the Fourier transform to be evaluated for each image, which becomes increasingly laborious for large

* Corresponding author.
** Permanent address: INSERM U. 138, Hôpital Henri-Mondor, F-94010 Créteil, France.

0304-3991/89/$03.50 © Elsevier Science Publishers B.V.
(North-Holland Physics Publishing Division)

data sets. Here, we present a way of expediting computation of the SSNR. In particular, we examine the properties of a reduced SSNR based on a limited number of partial sums, and conclude that a computationally much less demanding form of the SSNR may be defined that nevertheless retains essentially the full statistical precision of the original measure.

2. Basic definition

Given a set of images $\{x_{k,l}^{(i)}\}$ with corresponding Fourier transforms $\{X_{m,n}^{(i)}\}$, the SSNR ($\hat{\alpha}_R$) in a region R in Fourier space is given by:

$$\hat{\alpha}_R \triangleq \frac{\hat{\sigma}_{Rs}^2}{\hat{\sigma}_{Rn}^2/N} - 1. \tag{1}$$

The signal energy $\hat{\sigma}_{Rs}^2$ and the noise variance $\hat{\sigma}_{Rn}^2$, which is reduced by a factor N in the final average, are estimated as

$$\hat{\sigma}_{Rs}^2 = \frac{\sum_R |\bar{X}_{m,n}|^2}{n_R}, \quad \text{where} \quad \bar{X}_{m,n} \triangleq \frac{1}{N}\sum_{i=1}^{N} X_{m,n}^{(i)}, \tag{2}$$

$$\hat{\sigma}_{Rn}^2 = \frac{\sum_R \sum_{i=1}^{N} |X_{m,n}^{(i)} - \bar{X}_{m,n}|^2}{(N-1)n_R}; \tag{3}$$

n_R is the number of spectral components in R and $\bar{X}_{m,n}$ is the average image in Fourier space. The spatial frequency dependence of $\hat{\alpha}_R$ is calculated by taking R to be concentric annuli in Fourier space. An operational resolution limit is specified as the spatial frequency at which the SSNR falls below an acceptable baseline (typically, SSNR = 4). When the number of images to be included in the average is increased progressively, as is the case in most practical applications, the energy estimates in eqs. (2) and (3) may be updated recursively *, which is computationally more efficient than recomputing eqs. (1) to (4) for each addition to be data set.

3. Generalization to subsets

Instead of considering each image and its Fourier transform separately, let us consider n_g subsets of particles $\{x_{k,l}^{(i,j)}\}$, where $i = 1, \ldots, N_j$ and $j = 1, \ldots, n_g$, with a total of N images. The average over subset $\langle j \rangle$ is denoted by $\bar{x}_{k,l}^{\langle j \rangle}$ and its FT is $\bar{X}_{m,n}^{\langle j \rangle}$. In terms of these latter quantities, a reduced form of the SSNR may be computed as:

$$\hat{\alpha}'_R = \frac{\hat{\sigma}_{Rs}^2}{\hat{\sigma}_{Rn'}^2/N} - 1, \tag{4}$$

where $\hat{\sigma}_{Rs}^2$ is given by eq. (2) with the global average being evaluated as

$$\bar{X}_{m,n} = \frac{1}{N}\sum_{j=1}^{n_g} N_j \bar{X}_{m,n}^{\langle j \rangle}, \tag{5}$$

and where $\hat{\sigma}_{Rn'}^2$ is an estimate of the noise variance given by

$$\hat{\sigma}_{Rn'}^2 = \frac{1}{n_R(n_g - 1)} \sum_{(m,n)\in R} \sum_{j=1}^{n_g} N_j |\bar{X}_{m,n}^{\langle j \rangle} - \bar{X}_{m,n}|^2. \tag{6}$$

Note that the determination of eqs. (4)–(6) only requires the evaluation of n_g Fourier transforms, as opposed to N in the basic formulation.

4. Statistical analysis

Using the same arguments as in our previous study [1], $(\hat{\alpha}'_R + 1)$ can be shown to have a non-central F distribution with non-centrality parameter $\lambda = n_R \alpha_R$, where $\alpha_R = E\{\hat{\alpha}_R\}$, and degrees of

* This is achieved by defining the auxiliary arrays $\{\bar{X}_{m,n}^{(j)}\}$ and $\{\Phi_{m,n}^{(j)}\}$ which represent the Fourier transform of the average image and spectral density of the first j images, respectively. When adding the jth image to the previous data set of $(j-1)$ particles, these quantities are updated iteratively:

$$\bar{X}_{m,n}^{(j)} \triangleq \frac{1}{j}\sum_{i=1}^{j} X_{m,n}^{(i)} = \frac{(j-1)\bar{X}_{m,n}^{(j-1)} + X_{m,n}^{(j)}}{j},$$

$$\Phi_{m,n}^{(j)} \triangleq \frac{1}{j}\sum_{i=1}^{j} |X_{m,n}^{(i)}|^2 = \frac{(j-1)\Phi_{m,n}^{(j-1)} + |X_{m,n}^{(j)}|^2}{j}.$$

We also use the property that the numerator in eq. (3) is equal to

$$j\sum_R \left[\Phi_{m,n}^{(j)} - |\bar{X}_{m,n}^{(j)}|^2\right].$$

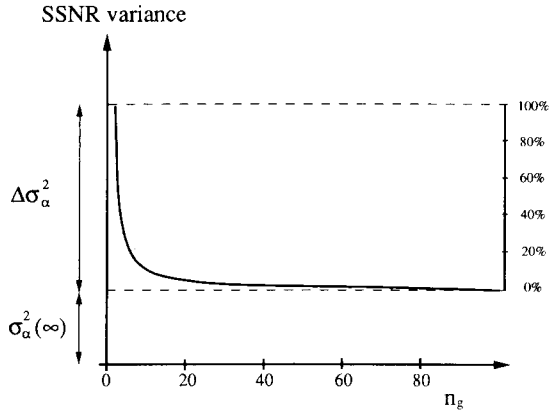

Fig. 1. Variance of the SSNR (α_R) as a function of the number of subsets (n_g) into which the data are partitioned.

freedom $n_1 = n_R$ and $n_2' = n_R(n_g - 1)$. Because $n_2' < n_2 = n_R(N-1)$, the estimate of the noise variance given by eq. (6) is less reliable than the standard estimate given by eq. (3), and so the reduced form of the SSNR will be subject to greater uncertainty. This effect may be quantified by using an approximate expression for the variance of a non-central F distribution [1] (see appendix), and making the appropriate substitutions for n_1 and n_2':

$$\mathrm{Var}\{\hat{\alpha}_R'\} = \frac{2+4\alpha_R}{n_R} + \frac{2+4\alpha_R+2\alpha_R^2}{n_R(n_g-1)}$$
$$= \sigma_\alpha^2(\infty) + \Delta\sigma_\alpha^2(n_g), \qquad (7)$$

where α_R denotes the true SSNR. The variance of the SSNR has been expressed as the sum of two terms, the first of which is independent of n_g, whereas the second decreases with n_g (the only parameter under direct control of the experimenter), as illustrated in fig. 1. The relative magnitudes of the two components shown in this plot are only illustrative since both depend on α_R, as well as on n_R, which varies with R and is fixed by sampling considerations. However, in all cases, the tendency is the same: as n_g increases, the variance decreases monotonically from $\sigma_\alpha^2(\infty) + \Delta\sigma_\alpha^2(2)$, for $n_g = 2$, to an asymptotic value of $\sigma_\alpha^2(\infty)$. Moreover, the relative proportion of the non-asymptotic variance component with respect to its maximum value (e.g. $\Delta\sigma_\alpha^2(n_g)/\Delta\sigma_\alpha^2(2)$) is a dimensionless quantity that is independent of both α_R and n_R and can be read in percents on the left axis of fig. 1. What is clearly illustrated by this graph is that the rate of improvement is much more substantial for smaller values of n_g than for larger ones. For practical purposes, we may tolerate an overall variance reduction that is slightly below the maximum achievable such as, for example, 90% (for $n_g = 11$) or 95% (for $n_g = 21$).

The statistical uncertainty in the SSNR (α_R) will translate into some corresponding uncertainty in spatial resolution. This relationship, however, is far from obvious and is highly dependent on the particular shape of a given SSNR curve, as discussed in the appendix.

5. Results and discussion

To investigate the effect that the number of subsets used may have on the SSNR resolution estimates, we tested two data sets: negatively stained ribosomal particles [6] and herpesvirus capsomers [7]. In each experiment, the images were randomly divided into n_g equal subsets and the resulting values of the reduced SSNR were calculated as described in section 3, the resolution (f_4) being determined at $\alpha_R = 4$ [1]. The procedure was repeated many times, and from these results, the expected value and standard deviation of f_4 were calculated for each n_g (tables 1 and 2). It is evident that, for both data sets, the standard deviation of f_4 decreases as n_g increases. The trend is essentially the same in both cases and is qualitatively consistent with the theoretical curve calculated for α_R (fig. 1). However, the relative proportion of the non-asymptotic variance component is surprisingly large, substantially greater than would be predicted from evaluating eq. (7) at the critical value of $\alpha_R = 4$. An explanation of this effect is that the resolution limit depends on the values of the SSNR over a range of frequencies and that the uncertainty in f_4 is determined predominantly by those spectral bins within this range that have the largest expected values for $\hat{\alpha}_R$ (cf. appendix). Another effect that can be observed is that the expected value of resolution limit slightly decreases as the number of groups increases. This

Table 1
Summary of an experiment in the statistical uncertainty in the spatial resolution specified by the SSNR for a set of $N = 80$ 40S ribosomal subunits images (size 64×64 and sampling step $\Delta x = 0.714$ nm) [6]; the data were divided into various numbers of subsets (n_g) with multiple such random divisions for each value of n_g

n_g	Number of trials	Range (nm^{-1})	Resolution limit (f_4)	
			Average (nm^{-1})	Standard deviation (%)
2	80	1/4.15–1/2.60	1/3.18	11.5
4	80	1/3.32–1/2.76	1/3.19	4.48
10	80	1/3.30–1/3.07	1/3.24	1.07
20	80	1/3.28–1/3.13	1/3.24	0.64
40	80	1/3.28–1/3.18	1/3.25	0.60
80	1	–	1/3.26	–

observation is consistent with the fact that the theoretical expected value of the SSNR curve can be shown to be slightly biased (in the proportion $n_2'/(n_2' - 2)$) and that this effect is the most pronounced for small values of n_g.

The partition of the data into two subsets only, which is the strategy that is used in both the DPR and the FRC, is clearly the worst case and the statistical errors in our examples are far from being negligible. In different trials, the resolution values given for the ribosomal data set varied from 2.6 to 4.1 nm depending simply on how the data were arbitrarily divided! A comparable span is encountered in resolution figures given by conventional FRC (which is mathematically related to SSNR with $n_g = 2$) and DPR [1]. However, these estimation errors fall off quite rapidly as n_g increases, and the statistical uncertainty for $n_g \geq 20$ should be rather close to that associated with our initial formulation of the SSNR criterion [1] ($n_g = N$).

Table 2
Summary of an experiment in the statistical uncertainty in the spatial resolution specified by the SSNR for a set of $N = 24$ herpesvirus capsomer images (size 50×50 and sampling step $\Delta x = 0.30$ nm) [7]; the data were divided into various numbers of subsets (n_g) with multiple such random divisions for each value of n_g

n_g	Number of trials	Range (nm^{-1})	Resolution limit (f_4)	
			Average (nm^{-1})	Standard deviation (%)
2	96	1/4.06–1/2.65	1/3.09	11.7
4	96	1/3.82–1/2.73	1/3.14	8.06
12	48	1/3.14–1/2.87	1/3.18	1.54
24	1	–	1/3.07	–

We would like to emphasize the distinction between the respective influences of N and n_g. Since the resolution is determined by the SSNR and noise is abated by increasing N, nominal resolution is usually improved by increasing N, although in practice the improvement to be achieved beyond a certain value of N is minimal [1]. On the other hand, the choice of n_g does not affect the resolution, but does affect the precision of our estimate of this quantity.

In section 3, we have not made any restrictions on the way we sub-divide the initial data set, and it can be shown that the expected value of the SSNR for a given n_g is independent of the number of images that have been assigned to each subset. However, from a practical point of view, it is preferable to use a balanced design (e.g. N/n_g particles per subset) in order to come up with partial averages that are comparable in the sense that they have identical statistical distributions.

Appendix. Uncertainty of the resolution estimate

To achieve some insight into the effects involved, we will make the simplifying assumption that the resolution limit always occurs within a sampling interval of some fixed discrete radial frequency f_0 at which the SSNR is determined. This is equivalent to requiring that $\alpha^+ = \alpha(f_0) \leq 4 \leq \alpha^- = \alpha(f_0 + \Delta f)$ and $f_0 \leq f_4 \leq f_0 + \Delta f$ and that these relations are also satisfied for all estimates of these quantities. In our initial formulation, the resolution limit f_4 is determined by linearly extrapolating the SSNR curve between f_0 and $f_0 + \Delta f$ and searching for the intersection with the critical value $\alpha = 4$. In this simplified case where the resolution limit always depends on the SSNR values evaluated at two discrete frequencies only, there is a direct relationship between the uncertainty in the determination of f_4, and the estima-

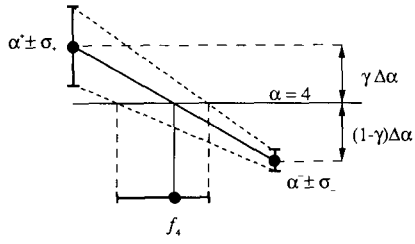

Fig. 2. Illustration of the how uncertainty in SSNR relates to uncertainty in the resolution estimate (f_4).

tion errors of α^+ and α^-, as illustrated in fig. 2. Using a first-order Taylor series expansion, it is relatively straightforward to derive the following equation:

$$\sigma_4 = \left|\frac{\partial\alpha}{\partial f}\right|^{-1} [\gamma\sigma_+ + (1-\gamma)\sigma_-] < \left|\frac{\partial\alpha}{\partial f}\right|^{-1} \sigma_+ \qquad (A.1)$$

where σ_4, σ_+ and σ_- are the standard deviations of $\hat{f}_4$, $\hat{\alpha}^+$ and $\hat{\alpha}^-$, respectively. $\partial\alpha/\partial f$ is the slope of the SSNR curve which is locally approximated by:

$$\partial\alpha/\partial f \cong -(\alpha^+ - \alpha^-)/\Delta f, \qquad (A.2)$$

and γ is a weighting factor lying between 0 and 1:

$$\gamma = (\alpha^+ - 4)/(\alpha^+ - \alpha^-). \qquad (A.3)$$

In most practical cases, this relationship is complicated since it involves values of the SSNR at more than two frequencies. However, based on eq. (A.1) we can make the following observations which will also apply, at least qualitatively, to less idealized cases:

(1) The standard deviation of the resolution estimate is inversely proportional to the slope of the SSNR curve.

(2) It is predominantly affected by the variability of the larger SSNR value α^+, which according to eq. (7) is greater than that of α. In particular, we note that for large values of α^+, the quadratic term in eq. (7) when n_g is small (e.g. $n_g = 2$) can be substantially greater than the asymptotic variance component which is a linear function of α^+. Fortunately, this term can be made arbitrarily small by selecting n_g sufficiently large.

References

[1] M. Unser, B.L. Trus and A.C. Steven, Ultramicroscopy 23 (1987) 39.
[2] J. Frank, Ultramicroscopy 1 (1975) 159.
[3] W.O. Saxton and W. Baumeister, J. Microscopy 127 (1982) 127.
[4] M. Kessel, M. Radermacher and J. Frank, J. Microscopy 139 (1985) 63.
[5] J.T. Finch, A. Klug and A.O.W. Stretton, J. Mol. Biol. 10 (1964) 570.
[6] J. Frank, A. Verschoor and M. Boublik, Science 214 (1981) 1353.
[7] A.C. Steven, C.R. Roberts, J. Hay, M.E. Bisher, T. Pun and B.L. Trus, J. Virol. 57 (1986) 578.